Layered antiferromagnetic spin structures of expanded face-centered-tetragonal Mn(001) as an origin of exchange bias coupling to the magnetic Co layer

Pin-Jui Hsu,[1] Chun-I Lu,[1] Yu-Hsun Chu,[1] Bo-Yao Wang,[1] Chii-Bin Wu,[1] Lun-Jia Chen,[1] Sheng-Syun Wong,[1] and Minn-Tsong Lin[1,2,*]

[1]*Department of Physics, National Taiwan University, Taipei TW-106, Taiwan*

[2]*Institute of Atomic and Molecular Sciences Academia Sinica, Taipei TW-106, Taiwan*

(Received 22 February 2012; published 29 May 2012)

Spin structures of an exchange-coupled-bilayer system of expanded-face-centered-tetragonal (e-fct) Mn(001) ultrathin films grown on Co/Cu(001) were resolved by means of spin-polarized scanning-tunneling microscopy. With an in-plane spin-sensitive probe, a layered antiferromagnetic-spin ordering of Mn overlayers was evidenced directly. In addition, the spin frustration across the same Mn layer creating a narrow domain wall down to nanometer scale was also observed along the buried step of Co underlayers. According to the micromagnetic simulation, the step-induced domain-wall width is in agreement with the experimental results. Such in-plane layered antiferromagnetic-spin structures of e-fct Mn(001) provide uncompensated spins at the interface with Co underlayers and elucidate the mechanism of the corresponding exchange-bias field observed in the previous studies.

DOI: 10.1103/PhysRevB.85.174434 PACS number(s): 75.50.Ee, 75.30.Gw, 75.70.Ak, 75.70.Kw

Exchange coupling between adjacent antiferromagnetic (AFM) and ferromagnetic (FM) layers has drawn much attention with regards to both fundamental magnetic physics[1,2] and the application of modern spintronic devices.[3,4] Typically, in the AFM/FM-bilayer systems, the exchange-coupling behavior could contribute the coercivity enhancement and the shift from the zero point of the field, which is the so-called exchange bias to the magnetic-hysteresis loops. According to previous studies,[1,2] two kinds of AFM-spin configurations, i.e., uncompensated and compensated, were proposed to explain such exchange-coupling behavior observed in the AFM/FM-bilayer systems. In the uncompensated-AFM-spin configuration, which provides the pinning effect of FM spins at the interface, the unidirectional anisotropy would be created to have FM magnetization rotated more easily in one direction. On the contrary, for the AFM layer with compensated-spin configuration in contact with the FM layer at the interface, different models, such as those for the formation of domains of the AFM layer,[5] noncollinear coupling at the interface,[6] and residual uncompensated spin from interfacial roughness,[7] etc., were reported. However, in these models, an interfacial-AFM-moment imbalance due to roughness or structural defects often has been introduced to create unidirectional interfacial energy by virtue of the coupling of the net uncompensated AFM moments with FM spins, which is actually the similar scenario described in the AFM layer with an uncompensated-spin configuration.

In the previous studies of the Mn/Co/Cu(001) system,[8] the expanded-face-centered-tetragonal (e-fct) Mn(001) films with a c/a ratio of 1.045 can be stably grown on the template of fct-Co(001) layers. From the magneto-optical Kerr effect (MOKE) measurements[8,9] of this AFM/FM-bilayer system, not only the coercivity enhancement but also the exchange-bias field have been observed. This was referred to as the antiferromagnetic properties of such e-fct Mn(001) coupled with ferromagnetic Co underlayers. In combination with the theoretical *ab initio* investigations of free-standing bulk tetragonal manganese[10] with a c/a ratio of 1.048, the in-plane $c(2 \times 2)$ compensated-antiferromagentic-spin structures of the e-fct-Mn(001)/Co/Cu(001) system have been suggested.[11,12] Therefore, the corresponding enhanced coercive field and exchange bias were attributed to the inevitable interface roughness or disorder,[6,13] creating a certain number of uncompensated spins at the interface such that the interfacial spins of the Co layer can be pinned to possess unidirectional anisotropy resulting in an exchange-bias field. However, in order to experimentally verify the proposed $c(2 \times 2)$ compensated-spin structure of e-fct Mn(001), the direct, advanced spin-mapping technique of spin-polarized scanning-tunneling microscopy (SP-STM)[14–17] is required.[11]

In contrast to the previous studies on body-centered-tetragonal (bct) Mn/Fe(001),[17–19] the e-fct-Mn/Co/Cu(001) system represents the important coercivity enhancement and prominent exchange-bias behavior due to interfacial coupling in the traditional AFM/FM ultrathin films, which is not observed in the bct-Mn/Fe(001) system. In order to answer the open question on the surface-spin structures of a few monolayers of e-fct Mn coupled to Co/Cu(001) and also have a general understanding of the physical origin of the exchange-bias field, a comprehensive study providing information on the connection to microscopic exchange-bias coupling and macroscopic magnetic behavior is significantly essential. Therefore, in this paper, we applied the SP-STM technique to resolve the spin structures of e-fct Mn(001) grown on Co/Cu(001), and the in-plane layered antiferromagnetic (LAF) spin arrangements have been observed. Besides, the AFM-coupling behavior of the Mn-capping layers was demonstrated to be connected with the determination of the coercivity enhancement observed in the thickness- and temperature-dependent-MOKE measurements. Furthermore, across the same Mn layer, the spin frustration accompanied with a sharp domain wall has been also observed in connection with hidden Co steps. The micromagnetic simulation for this AFM/FM-bilayer system further supports the picture of the LAF-spin structure of e-fct Mn(001).

The experiment was performed in an ultrahigh vacuum (UHV) multifunctional preparation chamber with a base pressure of about 3×10^{-11} mbar. The clean Cu(001) substrate was prepared by cycles of Ar^+ sputtering and annealing at 850 K. Both Mn and Co films were deposited at room temperature with a deposition rate of 60 ∼ 80 s/mL calibrated from STM. The measurement of low-energy-electron diffraction (LEED) was carried out to characterize the crystalline structure. From LEED-I/V curves (not shown here), the average vertical interlayer distance of the films was also determined using kinematic approximation.[20] Magnetic properties of the films were characterized by the *in situ* magneto-optical Kerr effect in the longitudinal geometry with a modulation and lock-in technique. As for the SP-STM measurements, the sample was transferred into a low temperature (LT)-STM chamber, which was cooled to 77.5 K, and the tungsten tip coated with 40-mL Fe was applied to provide in-plane spin sensitivity.[18,21] Furthermore, by adding a voltage modulation of 10 mV_{rms} to the sample bias, the conductance spectra can be obtained from the first harmonic signals detected by the lock-in amplifier.

In Fig. 1(a), the STM morphology of 5-mL Co grown on Cu(001) as well as the corresponding LEED patterns are shown. The surface morphology of Co films and $p(1 \times 1)$ diffraction pattern both illustrate the good epitaxial growth of the Co films. After 1.5 mL of Mn capped on 5-mL Co/Cu(001), not only the uncompleted first layer but also the start of the second Mn layer were observed from the STM morphology in Fig. 1(b). In addition, due to the room-temperature growth of Mn films, the first layer of the Mn-Co(001)-surface alloy was formed[22,23] according to the $c(2 \times 2)$ superstructure spots indicated by the black arrow in the inset LEED pattern, creating difficulties in separating spin from chemical contrast between the first and the second Mn layer by means of spin-resolved conductance-mapping measurements. Nevertheless, in the STM images of Figs. 1(c) and 1(d) with further Mn capping layers of 3.5 and 5.5 mL on 5-mL Co/Cu(001), there are no $c(2 \times 2)$ superstructures in appearance but only the $p(1 \times 1)$ layer left in the LEED patterns shown in both insets. This could be due to the fully outward buckling relaxation of Mn atoms after the completion of the first Mn layer, and no further interdiffusion of Co underlayers takes place at higher coverages of Mn films.[22,23] The STM images point out the smooth surface morphology of Mn films with respect to the two layers exposed to the top of the surface and give an indication of the two-dimensional layer-by-layer growth mode of Mn epitaxial films, also supporting the consistency reported previously.[22–24] For the vertical-interlayer-distance expansion of the e-fct-Mn films, a c/a ratio of ∼1.045 as the thickness of covered Mn layers of up to 3.5 mL has been confirmed and determined by either x-ray photoelectron-diffraction or LEED-I/V measurements.[8,9]

After we have realized the growth and crystalline structures of Mn films on Co/Cu(001), the SP-STM experiments at 77.5 K for resolving Mn surface-spin structures on this exchange-coupled AFM/FM-bilayer system are illustrated in the following. The topography and spin-resolved conductance-mapping image at a bias of −0.48 eV on 5.5-mL Mn/5-mL Co/Cu(001) are shown in Figs. 2(a) and 2(b), respectively. There exists an in-plane spin contrast between the fifth and the sixth Mn layer in SP-STM. Such a spin-mapping image illustrates the layered uncompensated spins at each

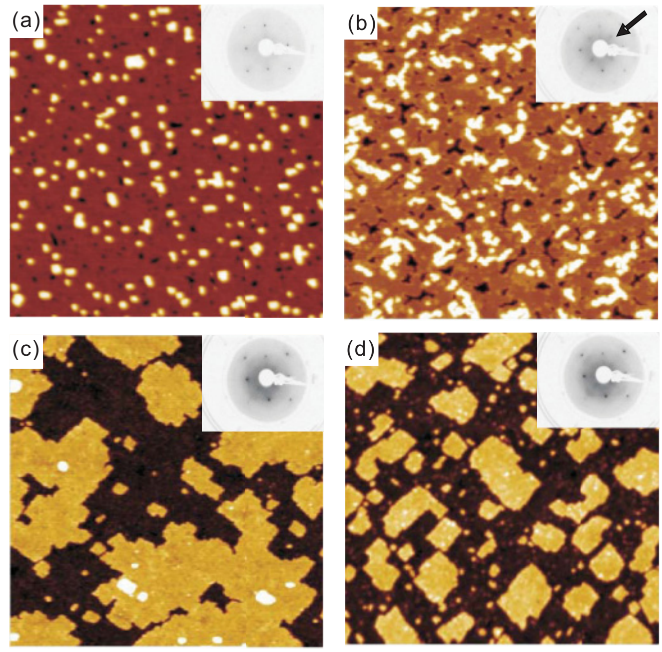

FIG. 1. (Color online) STM image taken at 77.5 K and the corresponding LEED patterns at 80 eV in the inset of (a) 5-mL Co/Cu(001), (b) 1.5-mL Mn, (c) 3.5-mL Mn, and (d) 5.5-mL Mn on 5-mL Co/Cu(001).

of the Mn surface layers rather than the proposed $c(2 \times 2)$ antiferromagnetic compensated-spin structures in the previous study.[11,12] Besides, in Fig. 2(c), showing full spectroscopy measurements, the spin-resolved-conductance spectra represent a spin-polarized surface-resonance state in the occupied density of states of the Mn layers. As compared to the studies in either Cr or Mn films grown on Fe(001) systems,[18,25] the spin-polarized surface-resonance state enables us to map out the surface-spin distribution of antiferromagnetic materials and is capable of providing a significant contribution to the magnetic asymmetry, i.e., defined as Eq. (1), which is demonstrated as the curve at the bottom of Fig. 2(c). Furthermore, in Fig. 2(e) together with the corresponding topography in the inset, we can even observe the in-plane antiparallel layered-Mn uncompensated-surface-spin structures in the place where there are multiple layers exposed to the surface. As a consequence, the in-plane LAF-surface-spin structures of the e-fct-Mn films coupled with adjacent Co layers have been resolved by SP-STM at 77.5 K:

$$A_{\text{symmetry}} \equiv \frac{dI/dV_{\text{parallel}} - dI/dV_{\text{antiparallel}}}{dI/dV_{\text{parallel}} + dI/dV_{\text{antiparallel}}}. \qquad (1)$$

In order to characterize the exchange-coupling behavior between the Mn and Co layers, the MOKE measurements were applied to investigate the temperature dependence of the coercivity on 5-mL Co/Cu(001) covered with Mn films. From Fig. 2(d), the coercivity field of 5-mL-Co films as a function of temperature was indeed obviously enhanced after capping with 5.5-mL-Mn layers. This demonstrates the antiferromagnetic property of e-fct-Mn films through the pinning effect on the interfacial spins of Co underlayers. Besides, in the reduced thickness of 3.5-mL Mn, the coercivity enhancement of 5-mL

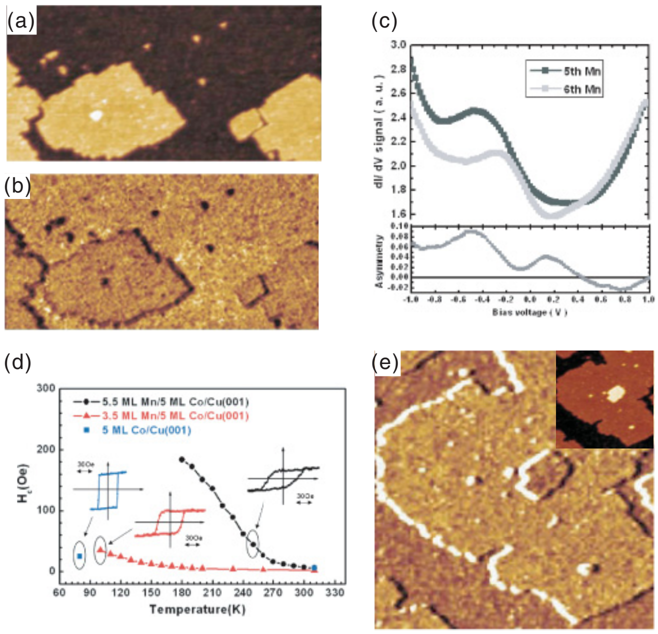

FIG. 2. (Color online) (a) STM morphology of 5.5-mL Mn capped on 5-mL Co/Cu(001). (b) The corresponding spin-mapping image. There is a color contrast between the fifth and the sixth Mn layer at the bias voltage of −0.48 V due to spin contrast. (Full spectrum set point: $U = 1.0$ V, $I = 1.0$ nA, and 100 nm × 50 nm) (c) Spin-resolved-conductance spectra and asymmetry are demonstrated. A spin-polarized surface-resonance state in the occupied density of states of the Mn layers has been found and has a significant contribution to the magnetic asymmetry. (d) The temperature and thickness dependence of MOKE measurements of the Mn/Co/Cu(001) system. The AFM behavior of the pinning effect on the interfacial spins of Co underlayers is demonstrated by the capped-Mn layers with thicknesses of 3.5 and 5.5 mL at low temperatures, respectively. (e) The spin mapping of the multilayers of Mn at the bias voltage 0.68 V. The in-plane layered-Mn uncompensated-surface-spin structures can still be observed, and the directions are individually antiparallel to each other.

Co remains observed at a low temperature around 110 K as compared to the pure 5-mL Co around 80 K, indicating that the pinning strength is still preserved in such thin Mn films. Therefore, in combination with the smooth surface morphology and the disappearance of the $c(2 \times 2)$ superstructures discussed above, surface-spin structures of 3.5-mL e-fct-Mn films are able to be resolved by the SP-STM at 77.5 K.

According to the topography and simultaneously obtained spin-mapping image of 3.5-mL Mn/5-mL Co/Cu(001) in Figs. 3(a) and 3(b), not only the LAF-spin structures but also the striking phenomenon of spin frustration across the same third Mn layer have been resolved. Similar to the e-bct-Mn films grown on the Fe(001) system,[26,27] the LAF-spin configuration can construct a prototypical model system to study topologically induced spin frustrations regarding the competition between domain-wall energy in AFM- and exchange-coupling energy in the interface of antiferromagnetism and ferromagnetism. As the region framed by the white-dashed square in Fig. 3(b), we show the averaged spin-resolved conductance-line profile in Fig. 3(c). The corresponding domain-wall width from spin frustration is able to be extracted through the standard wall-profile-fitting method for uniaxial systems:[28]

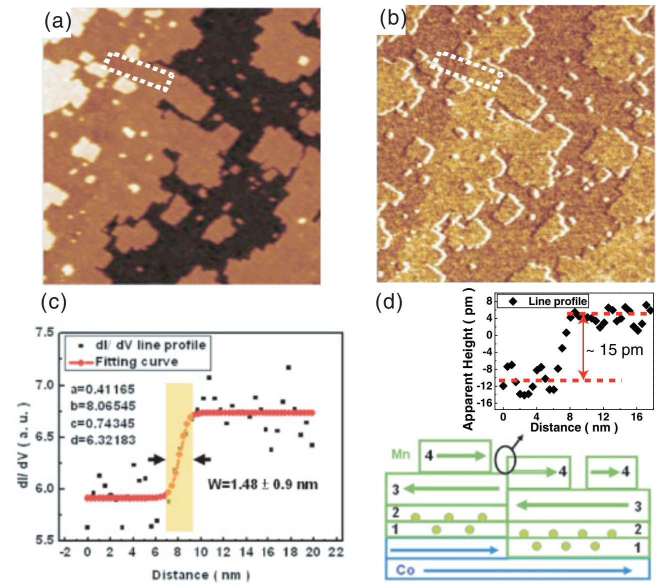

FIG. 3. (Color online) (a) The STM topography and (b) the corresponding spin mapping of 3.5-mL Mn on 5-mL Co/Cu(001). There is a spin frustration across the same Mn layer. (c) The averaged line profile of the spin-frustrated region framed by the white square in (b). Fitting via the domain-wall formula, a width of about 1.48 ± 0.9 nm could be obtained. (d) Topographic line profile, averaged over the region of the white-square frame in (a), is shown in the inset, and the schematic diagram of the spin-frustration phenomenon is also depicted. ($U = 0.6$ V, $I = 1.0$ nA, and 100 nm × 100 nm)

$$m(x) = a \tanh\left(\frac{x-b}{c}\right) + d, \tag{2}$$

where the domain-wall width is given by the parameter $2c$, and values of the best fitted parameters (a, b, c, and d) are shown in the inset of Fig. 3(c). The fitted domain-wall width from this formula is around 1.48 ± 0.9 nm, much smaller than the bulk domain-wall width in ferromagnets (∼200 nm) and antiferromagnets Cr(001) (∼120 nm).[29,30] Besides, as compared to the topography shown in Fig. 3(a), the spin-frustration phenomenon was found along the edge of the Mn films, and the topographic line profile of the same region with the spin-resolved conductance-line profile is depicted in the inset of Fig. 3(d). There is an apparent height difference of $\sim 15 \pm 1$ pm observed across the same third Mn layer, which is quantitatively equal to the out-of-plane lattice-constant difference between e-fct Mn (0.189 nm) and contracted face-centered-tetragonal (c-fct) Co (0.174 nm), obtained from the LEED-I/V measurements. Therefore, given the scheme illustrated in Fig. 3(d), the occurrence of spin frustration in layered antiferromagnetic-spin structures of e-fct-Mn films could be correlated with the buried Co steps underneath.

Since the resolution of lateral length is discussed on the nanometer scale, we can perform the micromagnetic simulation[31] based on the treatment of continuum micromagnetic theory to gain a further understanding of the LAF-spin configuration and spin frustration of e-fct-Mn films coupled with Co underlayers. In order to have a direct comparison between experimental and calculated results, the lateral size

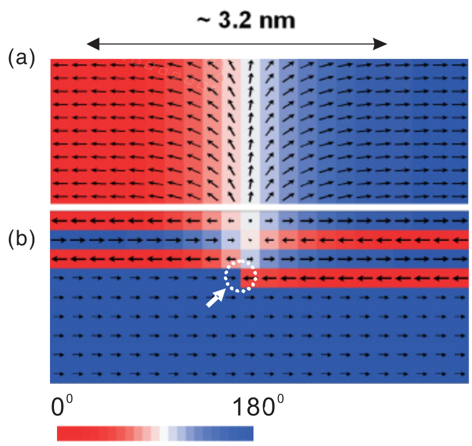

FIG. 4. (Color online) The simulation results of the (a) top view and (b) side view. The 3.5-mL Mn/5-mL Co/Cu(001) AFM/FM-exchange-coupled system is effectively fulfilled with a hidden Co step at the interface. There is a domain-wall width created in the spin frustration with the same order of magnitude as that of the experimental results.

of 100 nm × 100 nm was taken into account in the simulated model, which is the same with the observed STM image of Fig. 3(a). Besides, we gave the positive exchange interaction inside the whole Co FM domain and negative exchange interaction between each of the Mn layers with respect to the observed LAF-spin structures. Moreover, due to the LAF-spin structures of Mn films, we expected no stray field influence and ruled out the demagnetization-energy term. Thus, the total energy terms are composed of exchange and anisotropy energies in the simulation. As for the final magnetic-equilibrium state, it was obtained by calculating the lowest total energy as a function of the magnetization orientation under the constraint of constant magnetization. The material parameters of exchange stiffness (A_{ex}) and magnetocrystalline anisotropy (K_u) used in the simulation with the mesh unit cell of $0.2 \times 0.2 \times 0.2$ nm^3 are set in the following. $A_{ex} = 1 \times 10^{-11}$ J/m and $K_u = 4.1 \times 10^5$ J/m^3 were for Co (Ref. 32), and $A_{ex} = -1 \times 10^{-11}$ J/m and $K_u = 6 \times 10^4$ J/m^3 were for Mn. The magnetocrystalline anisotropy of Mn was deduced from the domain-wall width fitted by $2\sqrt{A_{ex}/K_u}$, and the uniaxial-anisotropy direction was parallel to the [110] easy-axis direction of the Co layers on Cu(001).

The simulated results are shown in the top and side views of Figs. 4(a) and 4(b), respectively. First of all, the LAF-spin structures of the Mn films can only be stabilized by coupling with the FM Co underlayers and cannot reach the equilibrium state if the Mn films are free standing without being pinned by Co underneath. Besides, the Co hidden step, indicated by the white arrow in Fig. 4(b), inducing spin frustration and thus creating the domain-wall width of ~3.2 nm, which is consistent with the value measured in the experiments, has been demonstrated in the top view of Fig. 4(a). We found the value of the domain-wall width is strongly correlated with the exchange-coupling strength between the Mn and Co layers and displays a broadening effect as the thicknesses of the Mn films increase. Such micromagnetic simulation illustrates the significance of the Co underlayers, which give rise to not only the LAF-spin structures of the Mn films through the magnetic direct-exchange coupling but also the spin-frustration phenomenon due to the buried steps. These recognize the good agreement with the observed experimental results and provide deeper understanding for the spin structure of the e-fct-Mn films coupled with the Co underlayers.

In conclusion, the in-plane LAF-spin structures of e-fct-Mn films grown on Co/Cu(001) have been resolved by SP-STM at 77.5 K. From the MOKE measurements, the coercivity enhancement as a result of the pinning effect on the interfacial spins of Co underlayers illustrates the AFM properties of e-fct-Mn films. In addition, the spin frustration across the same Mn layer induced by hidden Co steps not only supports the LAF-spin configuration but also indicates the magnetic-coupling competition between the domain-wall energy of the Mn layers and the exchange-coupling energy of the Mn/Co interface. The micromagnetic simulation recognizes the equilibrium state of the LAF magnetic structures of the Mn films coupled by the Co layers underneath and also the thickness-dependent domain-wall width created by buried Co steps, both of which are in agreement with the experimental measurements. Our findings demonstrate the exchange bias arising from the AFM/FM-exchange coupling instead of uncompensated spins from the interfacial roughness between the Mn and Co layers. This directly connects the microscopic AFM/FM-exchange coupling with the macroscopic-exchange-bias phenomenon, which can be taken as a significant step toward the general interpretation and can also shed light on the application of fabricating high-quality spintronic devices in the future.

This work was supported in part by the National Science Council of Taiwan through Grants No. NSC 99-2120-M-002-005 and No. NSC 100-2120-M-002-002.

*mtlin@phys.ntu.edu.tw

[1] J. Nogués and I. K. Schuller, J. Magn. Magn. Mater. **192**, 203 (1999).
[2] A. E. Berkowitz and K. Takano, J. Magn. Magn. Mater. **200**, 552 (1999).
[3] B. Dieny, V. S. Speriosu, S. Metin, S. S. P. Parkin, B. A. Gurney, P. Baumgart, and D. R. Wilhoit, J. Appl. Phys. **69**, 4774 (1991).
[4] D. Weller and A. Moser, IEEE Trans. Magn. **35**, 4423 (1999).
[5] A. P. Malozemoff, Phys. Rev. B **37**, 7673 (1988).
[6] N. C. Koon, Phys. Rev. Lett. **78**, 4865 (1997).
[7] K. Takano, R. H. Kodama, A. E. Berkowitz, W. Cao, and G. Thomas, Phys. Rev. Lett. **79**, 1130 (1997).
[8] J. T. Kohlhepp and W. J. M. de Jonge, Phys. Rev. Lett. **96**, 237201 (2006).
[9] J. T. Kohlhepp, H. Wieldraaijer, and W. J. M. de Jonge, Appl. Phys. Lett. **89**, 032507 (2006).

[10]J. Hafner and D. Spisak, Phys. Rev. B **72**, 144420 (2005).
[11]J. T. Kohlhepp, J. Phys. D **40**, 1300 (2007).
[12]J. T. Kohlhepp, O. Kurnosikov, and W. J. M. de Jonge, J. Magn. Magn. Mater. **286**, 220 (2005).
[13]A. P. Malozemoff, Phys. Rev. B **35**, 3679 (1987).
[14]S. Heinze, M. Bode, A. Kubetzka, O. Pietzsch, X. Nie, S. Blügel, and R. Wiesendanger, Science **288**, 1805 (2000).
[15]N. Berdunov, S. Murphy, G. Mariotto, and I. V. Shvets, Phys. Rev. Lett. **93**, 057201 (2004).
[16]C. B. Wu, P. J. Hsu, H. Y. Yen, and M.-T. Lin, Appl. Phys. Lett. **91**, 202507 (2007).
[17]U. Schlickum, W. Wulfhekel, and J. Kirschner, Appl. Phys. Lett. **83**, 2016 (2003).
[18]T. K. Yamada, M. M. J. Bischoff, G. M. M. Heijnen, T. Mizoguchi, and H. van Kempen, Phys. Rev. Lett. **90**, 056803 (2003).
[19]A. Tange, C. Gao, W. Wulfhekel, and J. Kirschner, Phys. Rev. B **81**, 220404(R) (2010).
[20]W. C. Lin, C. C. Kuo, C. L. Chiu, and M.-T. Lin, Surf. Sci. **478**, 9 (2001).
[21]M. Bode, Rep. Prog. Phys. **66**, 523 (2003).
[22]B.-C. Choi, P. J. Bode, and J. A. C. Bland, Phys. Rev. B **58**, 5166 (1998).
[23]B.-C. Choi, P. J. Bode, and J. A. C. Bland, J. Appl. Phys. **85**, 5063 (1999).
[24]B.-C. Choi, P. J. Bode, and J. A. C. Bland, Phys. Rev. B **59**, 7029 (1999).
[25]J. A. Stroscio, D. T. Pierce, A. Davies, R. J. Celotta, and M. Weinert, Phys. Rev. Lett. **75**, 2960 (1995).
[26]U. Schlickum, N. Janke-Gilman, W. Wulfhekel, and J. Kirschner, Phys. Rev. Lett. **92**, 107203 (2004).
[27]T. K. Yamada, E. Martínez, A. Vega, R. Robles, D. Stoeffler, A. L. Vázquez de Parga, T. Mizoquchi, and H. van Kempen, Nanotechnology **18**, 235702 (2007).
[28]A. Hubert and R. Schäfer, *Magnetic Domains* (Springer-Verlag, Berlin, 1998).
[29]E. Kneller, *Ferromagnetisms* (Springer-Verlag, Berlin, 1992).
[30]M. Kleiber, M. Bode, R. Ravlić, and R. Wiesendanger, Phys. Rev. Lett. **85**, 4606 (2000).
[31]The Object Oriented Micromagnetic Framework (OOMMF) Project at NIST. We used the OOMMF program Ver.1.2a3 [http://math.nist.gov/oommf/].
[32]X. Liu, M. M. Steiner, R. Sooryakumar, G. A. Prinz, R. F. C. Farrow, and G. Harp, Phys. Rev. B **53**, 12166 (1996).